Accepted Manuscript

Effects of post-processing on the thermomechanical fatigue properties of laser modified NiTi

B. Panton, A. Michael, Y.N. Zhou, M.I. Khan

Please cite this article as: Panton, B., Michael, A., Zhou, Y.N., Khan, M.I., Effects of post-processing on the thermomechanical fatigue properties of laser modified NiTi, *International Journal of Fatigue* (2017), doi: https://doi.org/10.1016/j.ijfatigue.2017.11.012

This is a PDF file of an unedited manuscript that has been accepted for publication. As a service to our customers we are providing this early version of the manuscript. The manuscript will undergo copyediting, typesetting, and review of the resulting proof before it is published in its final form. Please note that during the production process errors may be discovered which could affect the content, and all legal disclaimers that apply to the journal pertain.

Effects of post-processing on the thermomechanical fatigue properties of laser modified NiTi

B. Panton[1], A. Michael[1*], Y.N. Zhou[1], M.I. Khan[2]

[1]Centre for Advanced Materials Joining (CAMJ), University of Waterloo, 200 University Avenue West, Waterloo, ON, N2L 3G1, Canada

[2]Smarter Alloys, Inc., 75 Bathurst, Waterloo, ON, N2V 1N2, Canada

*corresponding author

e-mail: a2michae@uwaterloo.ca

phone: +1-519-888-4567 ext.36963

Abstract

The multifunctional capabilities needed for advanced shape memory alloys (SMA) actuators has been shown to be achievable by locally tuning the properties through laser processing. Before the wide-spread use of these SMAs is realized, a detailed understanding on the long-term stability and functional life span of these material must be achieved. The current study systematically investigates the effects of thermomechanical treatment on laser modified NiTi wires, while comparing them to the original base material. Surface analysis was done using a scanning electron microscope (SEM), while microstructure analysis was performed using transmission electron microscopy (TEM). Mechanical properties were assessed using standard tensile tests and a custom built thermomechanical fatigue. Results showed that the coarse-grains, large precipitates and surface defects associated with as laser modified NiTi resulted in reduced mechanical performance. However, subsequent thermomechanical treatment restored the refined microstructure and mechanical performance similar to the base material while providing the added functionality.

1.0 Introduction

Development of advanced materials such as shape memory alloys drives the next industrial revolution [1, 2]. These materials are used heavily in the medical and aerospace fields, and are seeing greater use as actuators across all industries [1, 3-5]. Their shape memory properties are key to creating new devices that were not previously possible. When these materials were initially developed they generally required only a few cycles of transformation where fatigue was not a problem, for applications such as orthodontic archwire [4], or a press-fit seal on a jet engine [5]. Relatively recent advancements in manufacturing of SMAs coupled with a greater understanding of the evolution of the material characteristics has led to the breakthrough of SMA actuators that can undergo millions of thermomechanical cycles before failure [6, 7].

There are a limited number of investigations into the thermomechanical fatigue of NiTi; due in part to the materials previous inability to reach high fatigue cycles. The benefits offered by SMA actuators over standard actuation devices have led to a rapid growth in the demand for SMA actuators by many sectors of industry [1-3]. This in turn has led to a recent increase in the investigation of the thermomechanical fatigue of SMAs [8-20], which was previously dominated by industry led research [6, 7].

The next generation of SMA manufacturing will produce components with multiple phase transformations [21-25]. Laser processing of SMAs is a key advancement in this area, which enables the local modification of properties by alteration of the chemistry [21, 22]. This has been used to create multiple memory actuators [21, 22], self-biasing actuators [26], and many other novel devices including the SmartArch[TM] a revolutionary orthodontic device. The only prior work on the effects of a pulsed laser on the thermomechanical fatigue of SMA wires was Panton et al.'s [27] study on laser welded NiTi. The current work presents the initial investigation of the

thermomechanical fatigue of laser modified SMA wires, as well as the ability of a cold-work and heat treatment regimen to improve thermomechanical fatigue lifespans and make them comparable to commercially available material.

2.0 Experimental procedures

2.1 Materials and Processing

The materials used in this investigation were a NiTi wire from Dynalloy Inc. with a diameter of 0.38 mm that was martensitic at room temperature. The 0.38 mm wire did not undergo any further processing before testing was performed, and is referred to as D38 for the remainder of the article. This wire is used for a comparison of the performance of the laser processed wires described below.

Additionally, a NiTi wire from Furukawa Electric Co. LTD. with a diameter of 0.70 mm that was pseudoelastic at room temperature was also used. This wire was modified to remove Ni and make the material martensitic at room temperature. Prior to processing no oxide removal was required, as it had previously been removed by the supplier [28]. The wire was cleaned with a regimen of acetone, ethanol, and water. Laser processing was performed using a Miyachi Unitek LW50A pulsed Nd:YAG laser, with a wavelength of 1.064 μm in an university test lab. During laser processing care was given to avoid excessive oxidation using argon gas shielding (flow rate of 25 CFH); however, slight surface oxidation was observed afterwards. The wires will be referred to as laser processed (LP) for the remainder of this study.

A set of the laser modified wires were subjected to a thermomechanical treatment process to reduce the grain size and reorient the texture [29, 30]. The wires were solutionized at 1000 °C for 3600 s followed by a water quench. Then they were cold worked through a series of reductions,

with an interannealing temperature of 600 ºC for 600 s, a total area reduction of 45 % after interannealing and a final heat treatment at 400 ºC for 3600 s. These wires had a final diameter of 0.46 mm and are referred to as the treated laser processed (T-LP) wires.

2.2 Phase and Fracture Analysis

An Olympus BX51M was used for optical microscopy. A JEOL 2010F TEM/STEM field emission microscope operating at 200 kV and a Phillips CM12 analytical TEM operating at 120 kV were used for TEM analysis. Fracture analysis was performed using a JEOL JSM-6460 SEM operated at 20 kV.

Differential Scanning Calorimetry (DSC) analysis was performed with a TA Discovery DSC equipped with a refrigerated cooling system. The DSC data was recorded from -75 ºC to 120 ºC using a controlled heating/cooling rate of 5 ºC/min. Analysis of the data was done using the TA Instruments Trios software v3.2 per the ASTM F2004-05(2010) standard.

2.3 Mechanical and Thermomechanical Testing

Tensile testing was performed using an Instron model 5548 micro-tensile tester that had a measurement accuracy of ±0.5 μm. An ASTM F216-07 test standard with extension rate of 1.0 mm/min and a gauge length of 25.1mm were used to test specimens.

Thermomechanical fatigue was performed using a custom setup as shown in Figure 1. Lead weights were used to subject a constant load (shown in Table 1) that was equivalent to a 600 MPa stress based on the nominal wire diameter. A gauge length of 25.1 mm was used for testing. The grips were faced with sacrificial pieces of ceramic to ensure there was no heatsink effect on the wire. The heating was performed at constant currents controlled by a Sorensen XG 33-25 power supply. These currents were set according to the recommended currents by Dynalloy Inc.

for wires of these diameters, as shown in Table 1. The current for the 0.70 mm diameter laser processed wire was determined by extrapolating the data provided by Dynalloy Inc. The current was delivered by speaker posts, shown in Figure 1. Heating was controlled to specific strain and thermally cycled until failure. Cooling was performed using a vortex tube that was turned on when the current was turned off. The setup measured the load using an Omega LCMFD 500 N load sensor and the displacement using a MT 2571 Heidenhain displacement sensor with a measurement sensitivity of ±0.2 μm. A NI PXI-1031 DAQ from National Instruments was used to monitor the sensors and control the power supply.

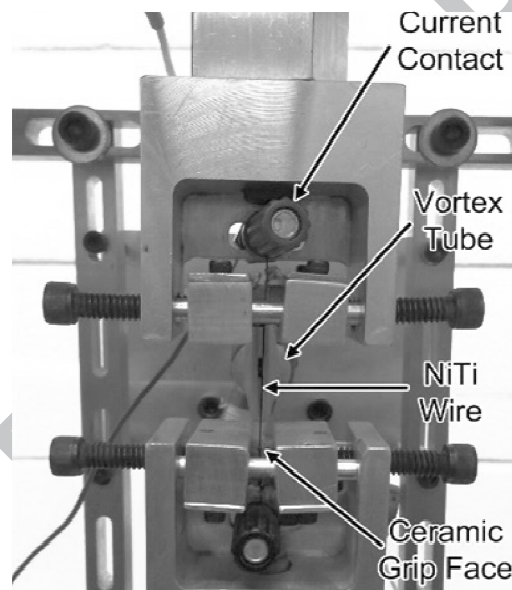**Figure 1: Thermomechanical fatigue tester.**

Table 1: Wire diameter, loads and currents used in the thermomechanical fatigue tests.

Wire	LP	T-LP	D38
Nominal Diameter (μm)	700	460	381
Constant Load (N)	241	100	68
Current (A)	7.43	3.27	2.25

3.0 Results and Discussion

3.1 Microstructure

The laser processing technique implemented in this study fully re-melted the work material. The centreline of the laser processed fusion zone was the weak point where failure occurred during initial wire drawing attempts. To avoid this, the fusion zone centrelines were partially removed by overlapping the laser processed spots by 60 %. The entire centreline could not be removed by increasing the overlap percentage, because this would result in an increase in Ni vaporization that would lead to Ti saturation and the formation of large amounts of Ti_2NiO_x phases. The laser processed microstructure is shown in Figure 2. Both the fusion boundary and the remaining centreline can be observed with the fusion zone being predominantly large columnar dendrites (see Figure 2), which is typical of welded NiTi wires [28, 31]. There is also a thin region of planar growth at the fusion boundary. Due to the relatively small cross sectional area of the wires, heat conduction away from the melt pool is restricted, which impedes the cooling rate in the fusion zone. The result is the planar growth at the fusion boundaries and the columnar dendrites in the fusion zone [28, 32, 33]. Epitaxial growth is also observed, as indicated by the dendritic grain that cross the fusion boundary (see Figure 2).
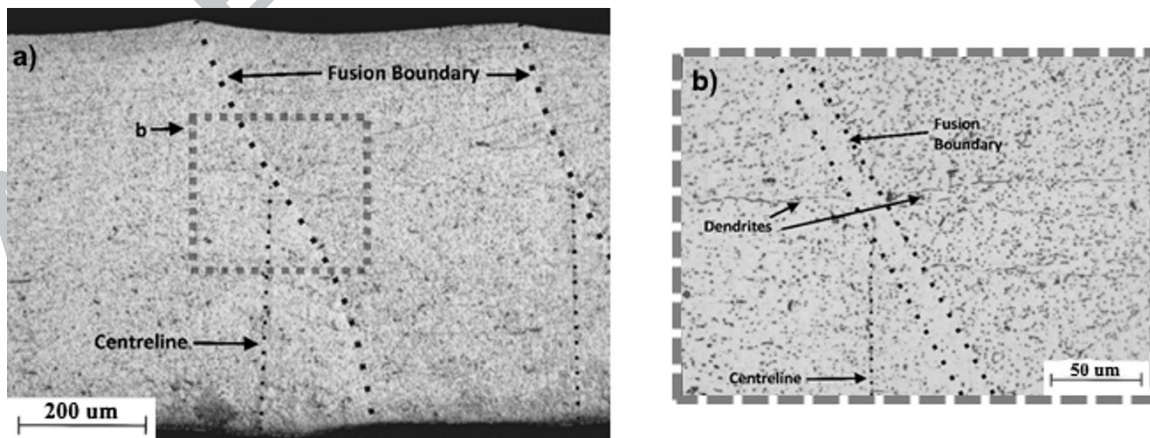

Figure 2: Optical micrograph of a) laser processed NiTi cross section and b) close-up of centerline partially overlapped by fusion zone.

The microstructure of the LP material is very coarse, with the grains and dendrites in the micron scale. TEM analysis of the LP sample is shown in Figure 3. The diffraction pattern shown in Figure 3a indicates that the material was in the B19' phase at room temperature. Figure 3b shows a large amount of Ti_2NiO_x present, due to the saturation of Ti in the matrix. Compositional analysis was used to confirm the identity of these inclusions. The Ti_2NiO_x phase was formed by microsegregation along the boundaries of the dendrites [34, 35]. It should be noted that these inclusions may be the result of oxide entrapment, the source of which could either be from the atmosphere (i.e. insufficient shielding) or pre-existing oxide on the sample surface.
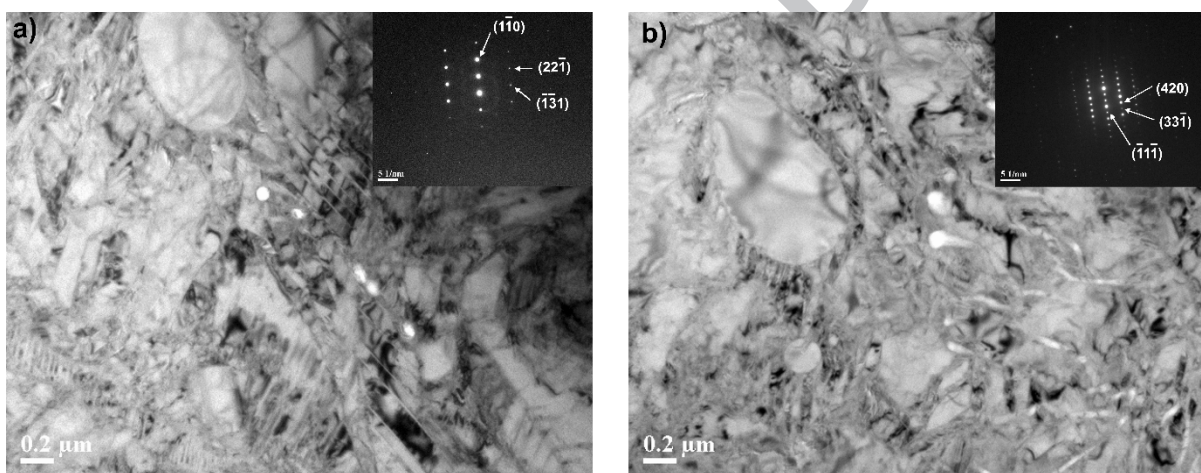

Figure 3: TEM a) of the LP twinned matrix and b) Ti_2NiO_x phase with in the matrix.

In comparison, the microstructure of the T-LP samples was a refined nanograined material, as shown in Figure 4. The average grain size measured via dark-field imaging was 29 nm. This grain size geometrically constricts the matrix such that the compound (001) twinning of nano-scaled microstructures formed (see Figure 4a), instead of the larger scale type I and type II twins (see Figure 3a) of the coarser microstructure that was observed in the LP sample [36]. During wire drawing, the Ti_2NiO_x inclusions were fractured and created particle-void-assemblies, as shown in Figure 4b.
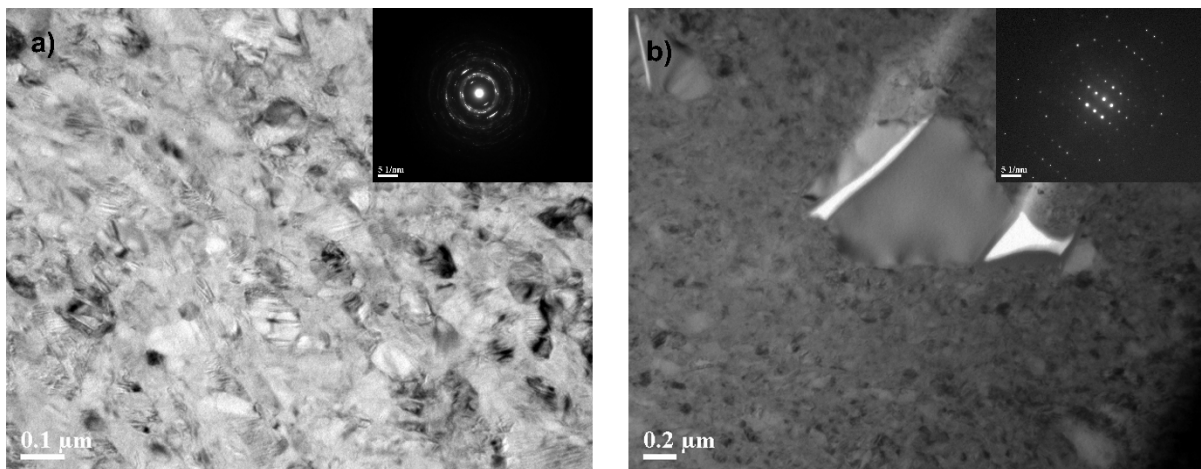
Figure 4: TEM of a) of the T-LP matrix and b) Ti$_2$NiO$_x$ particle void assembly.

TEM analysis of the microstructure of the D38 sample is shown in Figure 5. The average grain size as measured by dark-field TEM was 72 nm. This is typical of industrial NiTi designed for stability of actuation and long life. This Ti-rich material had no observed Ni$_4$Ti$_3$ precipitates, as these do not form in Ti-rich NiTi. Furthermore, no Ti$_2$NiO$_x$ and TiC inclusions were found in the TEM sample.
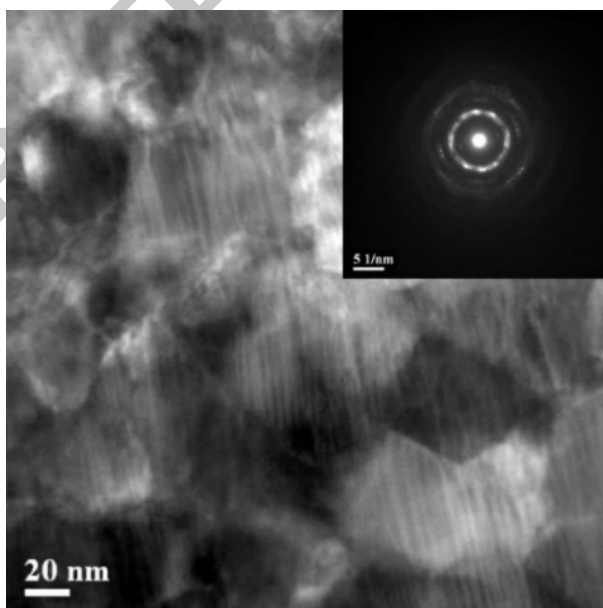

Figure 5: TEM of the nanocrystalline microstructure of the D38 sample.

3.2 Surface Properties

The surface properties of NiTi can affect the fatigue life of components [29]. This effect can become significant at smaller cross sectional sizes where defects become proportionally larger, and where the surface region becomes a large fraction of the cross-sectional area [29]. Figure 6 shows the SEM images of the surface of the LP, T-LP and D38 wires. Large cracks in the solidification surface are seen in the laser processed specimens, while the dominant feature in the wire drawn specimens is the striations. Qualitatively the T-LP wires are very similar to the D38 wires from the industry supplier. It follows that the effects of this surface would be similar to those seen in the industrial material.
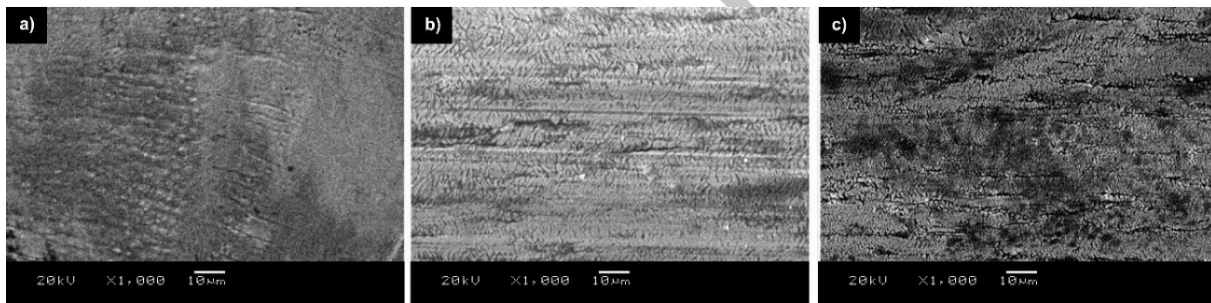

Figure 6: Surface of a) LP, b) T-LP and c) D38.

3.3 Thermal and Physical Properties

The DSC results are shown in Figure 7. The LP sample has a single-phase transformation typical of coarse-grained, low dislocation density and precipitate free NiTi [37]. The T-LP and D38 samples had similar phase transformation properties, a multi-stage phase transformation of a nanograined microstructure which geometrically constrained the martensite, reducing the maximum transformation strain, leading to the lower strain transformation of the R-phase [39]. The peaks of both these materials are in similar positions, indicating that they have similar compositions, and microstructures, which is confirmed by the TEM analysis discussed in the

previous section. The sharp peaks of the T-LP phase transformations indicate that the grains were dislocation lean [38]. The broad peaks of the D38 phase transformations indicate that the material had undergone training by the manufacturer to stabilize the microstructure by introducing dislocations to create networks [40, 41].
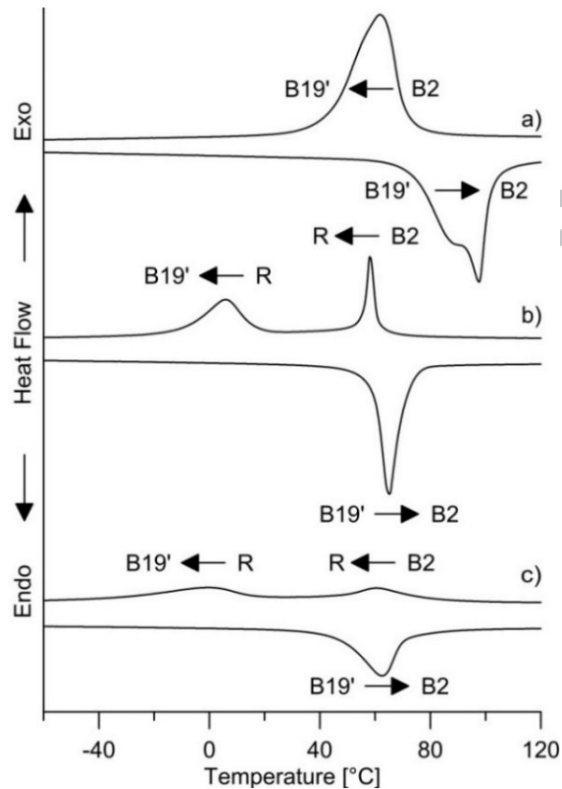

Figure 7: DSC analysis of a) LP, b) T-LP and c) D38.

The results of the tensile test pull-to-failure are displayed in Figure 8. The coarse-grained microstructure of the LP sample resulted in a lower UTS and ductility compared to the nanocrystalline T-LP sample. The T-LP and D38 had the same UTS, while the T-LP had a 34 % greater ductility than the D38, due to the smaller grain size [42].
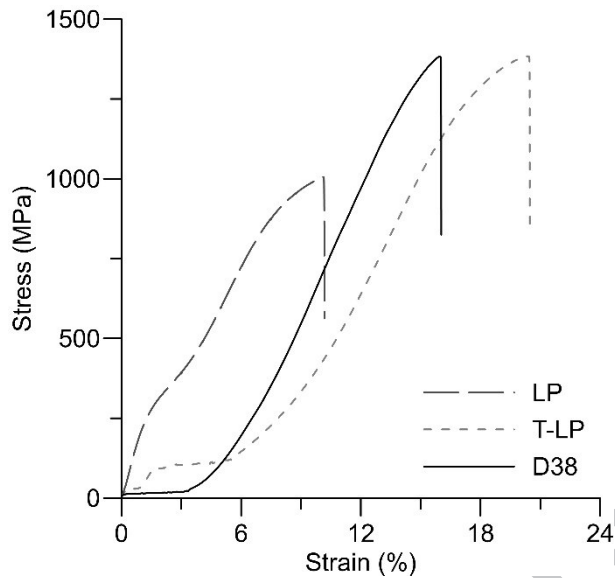
Figure 8: Tensile test pull-to-failure of the LP, T-LP and D38 at room temperature.

Additionally, the materials were tensile cycled to a load of 600 MPa and then thermally cycled at zero stress to recover shape memory strain, as shown in Figure 9. The coarse-grained LP sample had a significant plastic strain, and the ensuing plastic deformation resulted in a shape memory strain that was only 18 % the amount of the D38 material after 10 cycles. The T-LP sample had an increase in plastic strain compared to the LP sample, but achieved a shape memory strain equal to that of the D38 material. The smaller grains enabled a larger amount of deformation to occur than the coarser LP sample, but a significant part of this deformation was not recoverable due to the constriction of the matrix [43, 44]. The D38 wire had only 22 % of the plastic strain build-up that the T-LP sample experienced, but a similar shape memory strain. The training that the D38 material had undergone was used to build a dislocation network that ensured it would have a more stable initial deformation than the virgin, untrained T-LP sample, which was dislocation lean as indicated by the DSC curves in Figure 7.
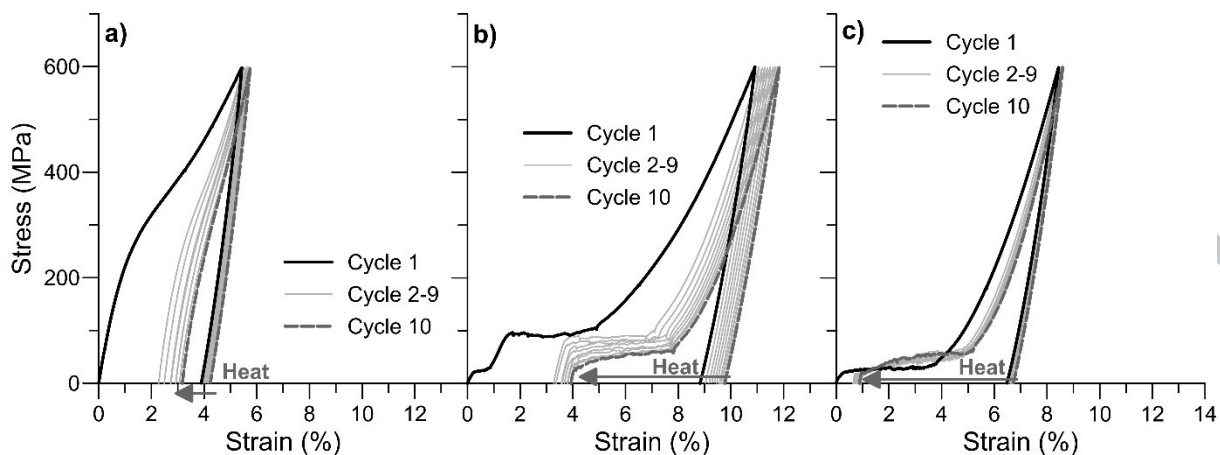
Figure 9: Tensile cycling to 600 MPa at room temperature, and zero-load shape memory recovery of a) the LP sample, b) the T-LP sample and c) the D38 sample.

3.4 Thermal and Physical Properties

Comparison of the fatigue lives of the LP, T-LP, and D38 are shown in Figure 10. The wires were loaded to 600 MPa and thermally cycled to controlled strains until failure. The coarse-grained LP sample was previously shown to have high plastic build-up and low shape memory strain which resulted in extremely low fatigue lives compared to the T-LP and D38 samples. The thermomechanical fatigue life of NiTi is related to the maximum achievable strain [12, 29]. The lower the percentage of the maximum strain used, the greater the fatigue life achievable. The maximum strains for 1 cycle at a load of 600 MPa are indicated on the strain axis (i.e. Y-axis) of Figure 10. The microstructure of the D38 material facilitated the maximum recoverable strain, followed by the more restricted, smaller grained T-LP sample, and finally the coarse-grained LP sample. At lower percentages of the maximum strain the T-LP and D38 had fatigue lives in the same order of magnitude.

The T-LP exhibited a substantial increase in both achievable strains and fatigue life at these higher strains compared to the LP sample. D38 showed a further increase in both achievable strain and fatigue life due to the more preferential grain size [12], and the training that it

underwent by the manufacturer [40, 41]. A training regime of 20 cycles at 4 % strain was applied to the T-LP material and resulted in an increase in the fatigue life from 21,474 cycles to 33,043 cycles at 2 % strain, which brings it close to parity with the D38 material that had an average cycle life of 36,022 cycles at 2 % strain, as shown in Figure 10. The stability of the microstructure ensured that progression of dislocations, and crack growth was slowed in the trained T-LP material, leading to the longer fatigue life than the LP material [12, 29].
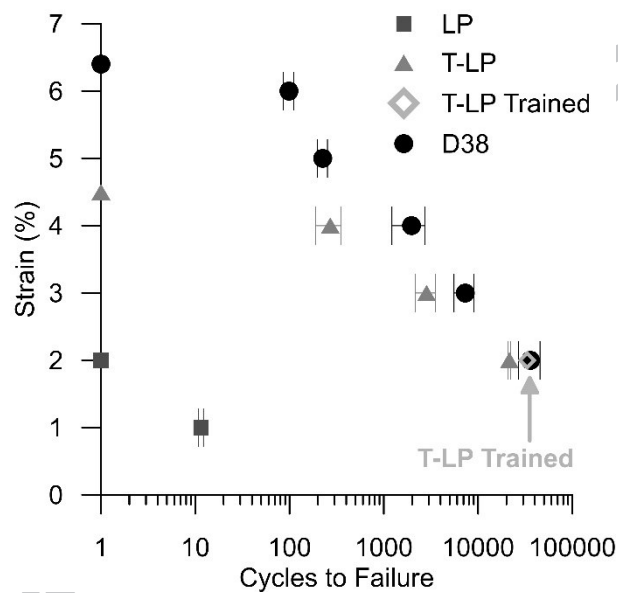

Figure 10: Cycles to failure of LP, T-LP, trained T-LP and D38 loaded to a constant 600 MPa and cycled to the indicated strains.

SEM images of the fatigue fractures are shown in Figure 11. The LP sample experienced a ductile rupture type failure that can be observed across the entire fracture surface, as shown in Figure 11a. The coarse-grained, precipitated and dislocation lean material underwent significant transformation induced plasticity in a small number of cycle, leading to this ruptured surface [8-12]. The T-LP and D38 samples have a small, distinct region where the crack initiated and propagated (see Figure 11b and c), with most of the surface having ductile rupture properties. The nanocrystalline material impeded the dislocation activity of transformation induced

plasticity, delaying crack initiation in these materials [45-47]. The majority of high cycle fatigue life in NiTi is in the crack initiation stage, with propagation occurring rapidly once the critical crack size is reached [48], which accounts for the uniformity of the fracture surfaces in Figure 11b and c. Brittle inclusions located at the surface serve as the crack initiation points [49].
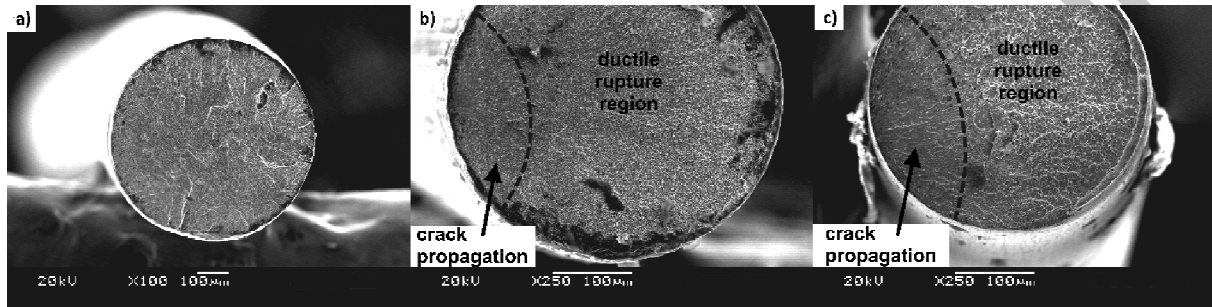

Figure 11: SEM images of fracture surfaces for a) LP (at 0.5 % strain), b) T-LP (at 2 % strain) and c) D38 (at 2 % strain) after cyclic fatigue testing.

4.0 Conclusions

Although the laser modified material exhibited reduced mechanical performance, subsequent thermomechanical treatment aided in restoring the properties while maintaining the added functionality. The T-LP material had the same UTS as the D38, but 34 % greater ductility due to the smaller grain size. Also, the T-LP had the same shape memory recovery strain as D38 when cycled to 600 MPa and thermally recovered at zero-load, however, the T-LP showed a 347 % greater plastic strain when compared to D38. The training of the D38 material by the manufacturer, and the less constrictive microstructure (slightly larger grains) of the D38 material ensured lower permanent deformation compared to the T-LP.

When loaded to 600 MPa, the coarse-grained and embrittled LP material had 1/3 of the recoverable strain of D38 and fatigue lives that were orders of magnitudes smaller. The T-LP had 2/3 of the maximum achievable strain of the D38, and fatigue lives in the same order of

magnitude as D38 at the lower strain values. The smaller grain size of the T-LP material limited the achievable strain. Training of the treated laser processed NiTi increased the fatigue life to parity with the D38 at 2 % strain. The current work demonstrates the feasibility of laser processed material matching the mechanical properties of commercially available alloys. Future work is underway to optimize the processing and training of laser modified NiTi to achieve superior fatigue properties.

Acknowledgements

References

1. J. Mohd Jani, et al., "A review of shape memory alloy research, applications and opportunities," *Materials and Design*, vol. 56, pp. 1078-113, 2014.

2. M. H. Elahinia, et al., "Manufacturing and processing of NitI implants: A review," *Progress in Materials Science*, vol. 57, pp. 911-946, 2012.

3. F. Butera, "Shape memory actuators for automotive applications," *Advanced Materials & Processes*, vol. 166, pp. 37-40, 2008.

4. T. Duerig, A. Pelton, D. Stöckel, "An overview of nitinol medical applications," *Materials Science and Engineering: A*, vol. 273-275, pp. 149-160, 1999.

5. D.J. Hartl, D.C. Lagoudas, "Aerospace applications of shape memory alloys," in *Proceedings of the Institution of Mechanical Engineers, Part G: Journal of Aerospace Engineering*, vol. 221, pp. 535-552.

6. A. Tuissi, et al., "Fabrication process and characterization of NiTi wires for actuators," SAES Getters, Milano, Italy, 2004.

7. L. Fumagalli, F. Buters, A. Coda, "SmartFlex® NiTi Wires for Shape Memory Actuators," *Journal of Materials Engineering and Preformance*, vol. 18, pp. 691-695, 2009.

8. S.K. Bhaumikm K.V. Ramaiah, C.N. Saikrishna, "Nickel-Titanium shape memory alloy wires for thermal actuators," in *Micro and Smart Devices and Systems*, K.J. Vinoy, Ed. Springer India, pp.181-198, 2014.

9. B. Kockar, et al., "Thermomechanical cyclic response of an ultrafine-grained NiTi shape memory alloy," *Acta Materialia*, vol. 56, pp. 3630-3646, 2008.

10. C.N. Saikrishna, et al., "Influence of stored elastic strain energy on fatigue behavior of NiTi shape memory alloys," *Materials Science & Engineering A*, vol. 587, pp. 65-71, 2013.

11. D. Wurzel, "Effects of different thermomechanical treatments on fatigue of NiTi shape memory alloys," *Journal De Physique IV*, vol. 11, pp. Pr8-535-Pr8-540, 2001.

12. J. Frenzel, et al. "Improvement of NiTi shape memory actuator performance through ultra-fine grained and nanocrystalline microstructures," *Advanced Engineering Materials*, vol. 13, pp. 256-268, 2011.

13. K. Gall, et al., "Effect of microstructure on fatigue of hot-rolled and cold-drawn NiTi shape memory alloys," *Materials Science and Engineering A*, vol. 486, pp. 389-403, 2008.

14. S. Belyaev, N. Resnina, A. Sibirev, "Peculiarities of the residual strain accumulation during thermal cycling of TiNi alloy," *Journal of Alloys and Compounds*, vol. 542, pp. 37-42, 2012.

15. X. Wu, K. Kutschej, A.C. Kneissi, "Study on the thermal fatigue of NiTi wires," *Zeitschrit fur Metallkunde*, vol. 94, pp. 122-126, 2003.

16. H. Meier, et al. "Smart Control Systems for Smart Materials," *Journal of Materials Engineering and Performance*, vol. 20, pp. 559-563, 2011.

17. R. Casati, A. Tussi, "Effect of current pulses on fatigue of thin NiTi wires for shape memory actuators," *Journal of Materials Engineering and Performance*, vol. 21, pp. 2633-2637, 2012.

18. K.V. Ramaiah, et al., "Fracture of thermally activated NiTi shape memory alloy wires," *Materials Science & Engineering A*, vol. 528, pp. 5502-5510, 2011.

19. D.C. Lagoudas, et al., "Thermomechanical fatigue of shape memory alloys," *Smart Materials and Structures*, vol. 18, pp. 1-12, 2009.

20. G. Scirè Mammano, E. Dragoni, "Functional fatigue of Ni-Ti shape memory wires under various loading conditions," *International Journal of Fatigue*, vol. 69, pp. 71-83, 2014.

21. M.I. Khan, A. Pequegnat, Y.N. Zhou, "Multiple memory shape memory alloys," *Advanced Engineering Materials*, vol. 15, pp. 386-393, 2013.

22. A. Pequegnat, et al., "Local Composition and microstructure control for multiple pseudoelastic plateau and hybrid self-biasing shape memory alloys," *Materials and Design*, vol. 92, pp. 802-813, 2015.

23. Y. Bellouard, et al. "Local annealing of complex mechanical devices: a new approach for developing monolithic micro-devices," *Materials Science and Engineering A*, vol. 273-275, pp. 795-798, 1999.

24. Q. Meng, et al., "Functionally graded NiTi strips prepared by laser surface anneal," *Acta Materialia*, vol. 60, pp. 1658-1668, 2012.

25. H. Scherngell, A.C. Kneissl, "Generation, development and degradation of the intrinsic two-way shape memory effect in different alloys systems," *Acta Materialia*, vol. 50, pp. 327-341, 2002.

26. B. Panton, Y.N. Zhou, M.I. Khan, "A stabilized, high-stress self-biasing shape memory alloy actuator," *Smart Materials and Structures*, vol. 25, 2016.

27. B. Panton, et al., "Thermomechanical fatigue of post-weld heat treated NiTi shape memory alloy wires," *Int. J. Fatigue*, vol. 92, Part 1, pp. 1-7, 11, 2016.

28. B. Tam, M.I. Khan, Y.N. Zhou, "Mechanical and functional properties of laser-welded Ti-55.8 wt pct Nitinol wires," *Metallurgical and Materials Transactions A*, vol. 42A, pp. 2166-2175, 2011.

29. S. W. Robertson, A. R. Pelton and R. O. Ritchie, "Mechanical fatigue and fracture of Nitinol," *International Materials Reviews,* vol. 57, pp. 1-37, 2012.

30. A. Pelton, "Nitinol Fatigue: A Review of Microstructures and Mechanisms," *Journal of Materials Engineering and Performance,* vol. 20, pp. 613-617, 2011.

31. H. C. Lin, S. K. Wu and J. C. Lin, "The martensitic transformation in Ti-rich TiNi shape memory alloys," *Materials Chemistry & Physics,* vol. 37, pp. 184-190, 1994.

32. C. W. Chan, H. C. Man and F. T. Cheng, "Fatigue behavior of laser-welded NiTi wires in small-strain cyclic bending," *Materials Science & Engineering A,* vol. 559, pp. 407-415, 2013.

33. S. Kou, *Welding Metallurgy.* Hoboken, NJ: John Wiley Sons, Inc., 2003.

34. A. Schuessler, T. Haas, P. Schlossmacher and H. Borgmann, "Micro Welding of NiTi Shape Memory Alloys," *Proc. Actuator 94: 4th Internat. Conf. on New Actuators, Bremen, June 15-17, 1994,* pp. S.372-376.

35. F. Sczerzenie, R. M. Manjeri, C. Belden and R. LaFond, "The effect of alloy formulation, cold work and inclusion content on micro-void formation in NiTi alloys," in *The International Conference on Shape Memory and Superelastic Technologies (SMST) may 12–16,* Pacific Grove, California, USA, 2014, pp. 17.

36. T. Waitz, V. Kazykhanov and H. P. Karnthaler, "Martensitic phase transformations in nanocrystalline NiTi studied by TEM," *Acta Materialia,* vol. 52, pp. 137-147, 2004.

37. K. Otsuka and X. Ren, "Physical metallurgy of Ti–Ni-based shape memory alloys," *Progress in Materials Science,* vol. 50, pp. 511-678, 2005.

38. A. R. Pelton, G. H. Huang, P. Moine and R. Sinclair, "Effects of thermal cycling on microstructure and properties in Nitinol," *Materials Science & Engineering A,* vol. 532, pp. 130-138, 2012.

39. T. Waitz, T. Antretter, F. D. Fischer and H. P. Karnthaler, "Size effects on martensitic phase transformations in nanocrystalline NiTi shape memory alloys," *Materials Science and Technology,* vol. 24, pp. 934-940, 2008.

40. C. N. Saikrishna, K. V. Ramaiah and S. K. Bhaumik, "Effects of thermo-mechanical cycling on the strain response of Ni-Ti-Cu shape memory alloy wire actuator," *Materials Science & Engineering A,* vol. 428, pp. 217-224, 2006.

41. B. Erbstoeszer, B. Armstrong, M. Taya and K. Inoue, "Stabilization of the shape memory effect in NiTi: an experimental investigation," *Scripta Materialia,* vol. 42, pp. 1145-1150, 2000.

42. J. Schaffer, "Structure-Property Relationships in Conventional and Nanocrystalline NiTi Intermetallic Alloy Wire," *Journal of Materials Engineering and Performance,* vol. 18, pp. 582-587, 2009.

43. E. Polatidis, N. Zotov, E. Bischoff and E. J. Mittemeijer, "The effect of cyclic tensile loading on the stress-induced transformation mechanism in superelastic NiTi alloys: an in-situ X-ray diffraction study," *Scripta Materialia,* vol. 100, pp. 59-62, 2015.

44. R. Delville, B. Malard, J. Pilch, P. Sittner and D. Schryvers, "Microstructure changes during non-conventional heat treatment of thin Ni–Ti wires by pulsed electric current studied by transmission electron microscopy," *Acta Materialia,* vol. 58, pp. 4503-4515, 2010.

45. G. Eggeler, E. Hornbogen, A. Yawny, A. Heckmann and M. Wagner, "Structural and functional fatigue of NiTi shape memory alloys," *Materials Science and Engineering: A,* vol. 378, pp. 24-33, 2004.

46. C. Saikrishna, K. Ramaiah, S. Allam Prabhu and S. Bhaumik, "On stability of NiTi wire during thermo-mechanical cycling," *Bulletin of Materials Science,* vol. 32, pp. 343-352, 2009.

47. K. N. Melton, "Ni-Ti based shape memory alloys," in *Engineering Aspects of Shape Memory Alloys*Anonymous London: Butterworth-Heinemann, 1990, pp. 21-35.

48. A. Wick, X. Y. Gong, J. Fino, J. Sheriff and A. R. Pelton, "Bending fatigue characteristics of nitinol," in *Proc. ASM Materials & Processes for Medical Devices Conf.* Minneapolis, MN, USA, August 2004, pp. 15-20.

49. E. Hornbogen, "Review Thermo-mechanical fatigue of shape memory alloys," *Journal of Materials Science,* vol. 39, pp. 385-399, 2004.

Highlights

- Laser processing was used to locally tune the material composition
- Microstructural analysis detailed the changes after laser processing and thermomechanical treatments
- Mechanical performance was evaluated and compared to microstructure
- Fatigue performance of laser tuned NiTi wires was comparable to commercially available wires after thermomechanical treatments